Geophys. J. Int. (2004) **157,** 164–174 doi: 10.1111/j.1365-246X.2004.02177.x

The earthquake and tsunami of 1865 November 17: evidence for far-field tsunami hazard from Tonga

Emile A. Okal,[1] José Borrero[2] and Costas E. Synolakis[2]

[1]*Department of Geological Sciences, Northwestern University, Evanston,* IL 60201, *USA. E-mail: emile@earth.nwu.edu*
[2]*Department of Civil Engineering, University of Southern California, Los Angeles,* CA 90089, *USA*

Accepted 2003 October 10. Received 2003 September 20; in original form 2003 April 9

SUMMARY

Historical reports of an earthquake in Tonga in 1865 November identify it as the only event from that subduction zone which generated a far-field tsunami observable without instruments. Run-up heights reached 2 m in Rarotonga and 80 cm in the Marquesas Islands. Hydrodynamic simulations require a moment of 4×10^{28} dyn cm, a value significantly larger than previous estimates of the maximum size of earthquake to be expected at the Tonga subduction zone. This warrants an upwards re-evaluation of the tsunami risk from Tonga to the Cook Islands and the various Polynesian chains, which had hitherto been regarded as minor.

Key words: historical earthquakes, Tonga Islands, tsunami hazard, tsunami simulation.

1 INTRODUCTION

Among large earthquakes recorded from the Tonga–Kermadec arc system, the only report of tsunami waves observed in the far field with metric amplitudes, and thus prone to inflicting damage, is from an earthquake in Tonga in 1865 November (Solov'ev & Go 1984). In particular, it is remarkable that the large earthquakes of 1917 May 1 in Kermadec, 1917 June 26 in Samoa and 1919 April 30 in Tonga, to which Gutenberg & Richter (1954) assigned magnitudes of 8.6, 8.7 and 8.4 respectively, generated only local tsunamis which failed to export death and destruction across the Pacific Basin. At most, the three events (and many smaller ones from the same region) were recorded on distant tidal gauges at decimetric level or below. There is a lone report (Angenheister 1921) of one Hawaiian bay being drained and undergoing oscillations following the 1919 event, but the timing (between 07:30 and 10:30, Hawaiian time, i.e. between 18:00 and 23:00 GMT) is late by 4.5 hr.

The failure of these three supposedly gigantic events to generate transoceanic tsunamis is supported by the seismic moment estimates of Okal (1992), 1.6×10^{28}, 1.3×10^{28} and 2.5×10^{28} dyn cm respectively, based on mantle magnitudes. These figures, and other reassessments of the size of historical earthquakes (Abe 1981), have led to the perception of the 1919 event as the maximum size earthquake to be expected in the Tonga–Kermadec province. This result is generally supported by the observed correlation between the maximum size of interplate earthquakes and the strength of coupling at the trench, as expressed by the combination of the inverse age of the subducting lithosphere and the convergence rate between the two plates (Uyeda & Kanamori 1979; Ruff & Kanamori 1980). In the case of Tonga, the large age of the subducting lithosphere (typically 120 Ma) trades off with the relatively fast kinematic rate (quoted by Ruff & Kanamori at 8 cm yr^{-1}) to yield a moderate maximum event size, dwarfed by the mega-thrust earthquakes documented at such young, fast-sinking subduction zones as Chile or Peru.

However, recent measurements using space geodesy techniques have found evidence for considerable backarc spreading in the Lau Basin, and consequently a convergence rate as large as 16 cm yr^{-1} at the latitude of Tongatapu, and a record 24 cm yr^{-1} at the northern end of the arc (Bevis *et al.* 1995). In turn, such revised rates may compensate for the greater age of the subducting lithosphere in Tonga, and still result in a largely coupled subduction zone with the potential for much larger earthquakes casting enhanced tsunami hazard across the Pacific Basin. If confirmed, this would warrant a substantial reassessment of tsunami risk in locations such as the Cook Islands, French Polynesia and possibly even Easter Island.

In this framework, the present paper addresses the question of the probable size of the 1865 earthquake, based on forward modelling of the reported run-up at Rarotonga and Nuku Hiva. We conclude that the earthquake probably had a moment of 4×10^{28} dyn cm, i.e. significantly larger than its 1919 counterpart, the latter possibly featuring a deeper than normal focus.

2 LOCATING AND INTERPRETING THE 1865 EVENT

2.1 The earthquake

The 1865 earthquake is reported in a number of publications (Fuchs 1866; Perrey 1867; Rudolph 1887, p. 358; Krümmel 1911, p. 142) which essentially consist of different wordings of the same original evidence, namely reports from ship captains. On their basis, it is possible to piece together the following interpretation: the strongest shock originated around 05:40 to 06:00, and was strongly felt from Vava'u in the north (18.7°S; see Fig. 1) to Ha'apai in the south

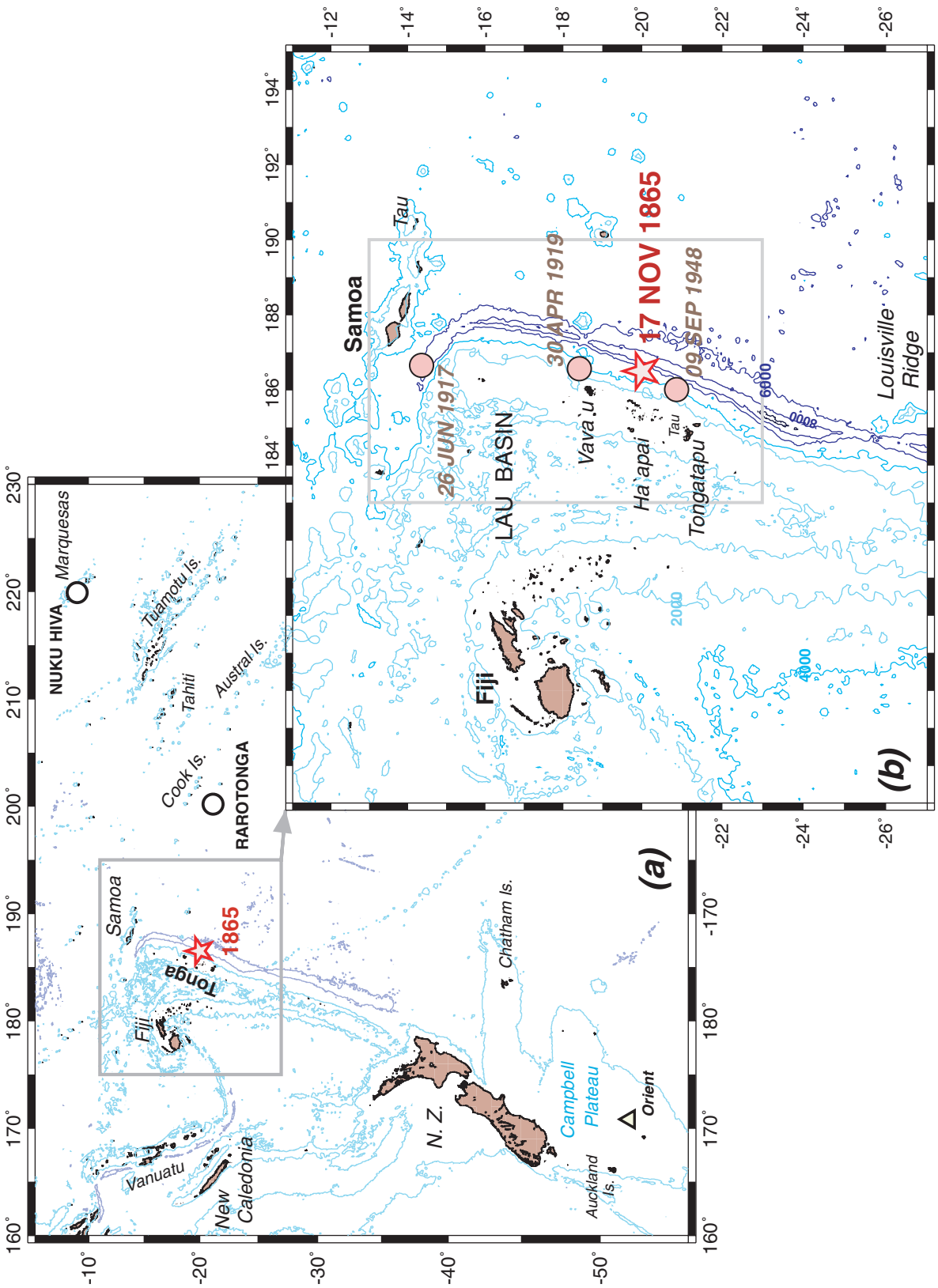

Figure 1. (a) Location map of the study area in the southwestern Pacific. Bathymetric contours are drawn at 2000 and 6000 m. The star is at the probable location of the 1865 earthquake. The open circles show the locations of tsunami reports, on the islands of Rarotonga (Cook) and Nuku Hiva (Marquesas). The open triangle shows the reported position of the *Orient* (see Appendix). (b) Close-up of the Tonga arc and trench. The circles show the relocated epicentres of the 1917, 1919 and 1948 events. The star is the probable epicentre of the 1865 shock. Isobaths are drawn at 2000-m intervals. The grey box outlines the region shown in Fig. 2.

(20.0°S). There are reports of the earthquake being felt on ships at sea as far south as 24°S. An intriguing report from 51°S (Barry 1866) is probably purely coincidental (see the Appendix).

Rudolph (1887) reports that the event was felt starting at 04:20 by the English ship *John Wesley*, which hit a coral reef in the vicinity of Tau, the easternmost island in the Samoa group (14.2°S, 169.5°W), and that the ship later capsized during the main shock at 06:00. Should this location be confirmed, that would suggest an extensive area of high intensities for the event, and so most probably an elongated rupture zone extending some 600 km from Ha'apai in the south to the northern corner of the Tonga trench, at 15°S. We regard this as unlikely, and rather believe that Rudolph (1887) confuses the island of Tau in Samoa with the small islet of Tau (21.02°S, 175.02°W), part of the coral reef of Tongatapu (Fig. 1). Indeed, Tau (Samoa) is at least 250 km from the nearest point on the plate boundary, and would be an unlikely venue to feel what appears to be a small foreshock at 04:20, much more likely to have occurred in the vicinity of Tau (Tonga). It is therefore probable that the earthquake was felt strongly only in the Tonga Islands, but throughout their group. This is in contrast to the case of the 1919 event, relocating at 18.42°S in the north of Tonga (see below), and reported as being felt only weakly in Tongatapu (Solov'ev & Go 1984).

The date of the events is given in all sources as 1865 November 18, with times most probably local. It is impossible to assert beyond doubt which exact time was being used in the various islands in 1865, and so we will assume that this represents solar time, which is probably not wrong by more than 2 hr. It is also most probable that the islands in question, all initially colonized by British settlers travelling eastwards, were observing the European day reckoning (note in particular that Samoa changed its calendar to the American reckoning only in 1892), and hence that the origin of the earthquake (05:40 local time) should be around 17:10 on 1865 November 17, in universal (GMT) time. We therefore use this date in the title of the present paper, and hereafter when referring to the 1865 earthquake.

2.2 The tsunami

There exist two independent reports of a far-field tsunami which can be correlated with the 1865 Tonga earthquake:

At Avarua, Rarotonga, the above sources, based on a letter to *Le Messager de Tahiti*, and summarized by Solov'ev & Go (1984), mention a series of three regressions and rises of the sea, ranging between 1.2 m below the low-tide mark and 1.2 m above the high-water mark, during a period reported as being low tide. The fluctuations in sea level did not feature individual waves but rather involved the whole mass of the sea oscillating slowly and calmly. It is obvious that these descriptions fit the characteristics of a tsunami reaching a distant harbour. The phenomenon started at 09:20 on November 18 and lasted about half an hour. The traveltime of a tsunami from the estimated epicentre (20°S, 173.5°W) to Rarotonga is 1 hr 40 min, which would put the first wave at 08:30 solar time at Rarotonga (longitude 159°W), the 50-min difference with the reported time more than likely expressing the uncertainties in the time conventions in use on the various islands. However, there is some confusion, since modern tidal calculations predict a high tide of moderate amplitude (+20 cm) at the reported time of arrival of the wave (H. Mofjeld, personal communication, 2003). We can offer no explanation for this discrepancy, but we circumvent the problem by assessing the total range of the wave's oscillation, which amounts to 3.3 m, given the observed modern-day difference of 90 cm between extreme low and high tides. Anticipating on the results of our simulations, we partition this total amplitude asymmetrically (+2 m and −1.3 m); note that the resulting amplitude of 2 m is compatible with the report of a low tide. In other words, if the tide had really been high at that time, to the extent that the run-up above tide level had been no more than, say, 1.2 m, then the expected down-draw during regression would have been at most 80 cm, from *high* tide, which would not have significantly exposed the bottom below the low-water mark, contrary to the reports in Solov'ev & Go (1984), thus bringing a second contradiction to this report.

At Taiohae, on the island of Nuku Hiva in the Marquesas, Lawson (1869) compares the event of 1865 with the great Arica, Peru (now Chile) tsunami of 1868 which had reached 4 m above high tide, and destroyed many houses on the beach:

'The earthquake in Tonga, three or four years ago, was felt [sic] the same day at two o'clock in the afternoon, and ended around six o'clock; but this time, the sea rose only to the level of the highest tides, approximately every fifteen to twenty minutes [. . .] this was not felt in Tahiti and neighbouring areas.'

We computed a tsunami travel time of 4 hr 40 min from the estimated epicentre (20°S, 173.5°W) to Nuku Hiva, which would suggest a first arrival of the tsunami at 21:50 GMT, or 12:30 solar time in the Marquesas (longitude 140°W). Given the uncertainties on the nature of the time reported, the agreement with Lawson's (1869) observation (2 p.m.) must be regarded as excellent. In order to estimate the run-up, we first note that the amplitude of maximum high water at Taiohae is 1.65 m; also, the tide is on the average 6 hr late relative to Rarotonga; taking into account the additional 3 hr of transit of the tsunami, we conclude that the tsunami reached Nuku Hiva during an episode of ebbing tide, with sea level probably between 70 and 100 cm, suggesting in turn a run-up of 65 to 95 cm. These numbers (on the average 80 cm) should not be considered more than an order of magnitude; they should be interpreted to reject both significantly lower values of the run-up in Taiohae Bay (e.g. 30 cm) which would probably have remained undetected except during a very high tide, as well as much larger values (e.g. 1.5 m or more), which would require a clear overflow of the high-water mark, contrary to the testimony of Lawson (1869).

We conclude that the independent evidence reported at Rarotonga and the Marquesas leaves no possible doubt as to the direct association of the waves with the Tongan earthquake. To our best knowledge, this is the first confirmed report of an earthquake in Tonga generating a tsunami detectable other than instrumentally in the far field.

3 RELOCATION OF INSTRUMENTAL EVENTS

The goal of this section is to optimize the probable location of the 1865 event, in order to build source models to be used in the hydrodynamic simulations in Section 4, for both the 1865 event and the more recent 1919 shock for which no tsunami is reported in the far field. For this purpose, we first discuss the background seismicity and in particular the large historical earthquakes of 1917, 1919 and 1948 in the same general area, which we proceed to relocate based on arrival times reported by the International Seismological Summary (ISS). We use the interactive iterative procedure of Wysession *et al.* (1991), which includes a Monte Carlo algorithm injecting Gaussian noise into the data set in order to obtain confidence limits for the relocated epicentres. For the old events (1917, 1919) considered here, we use a standard deviation $\sigma_G = 15$ s for the Monte Carlo noise, but only $\sigma_G = 3$ s for the 1948 shock.

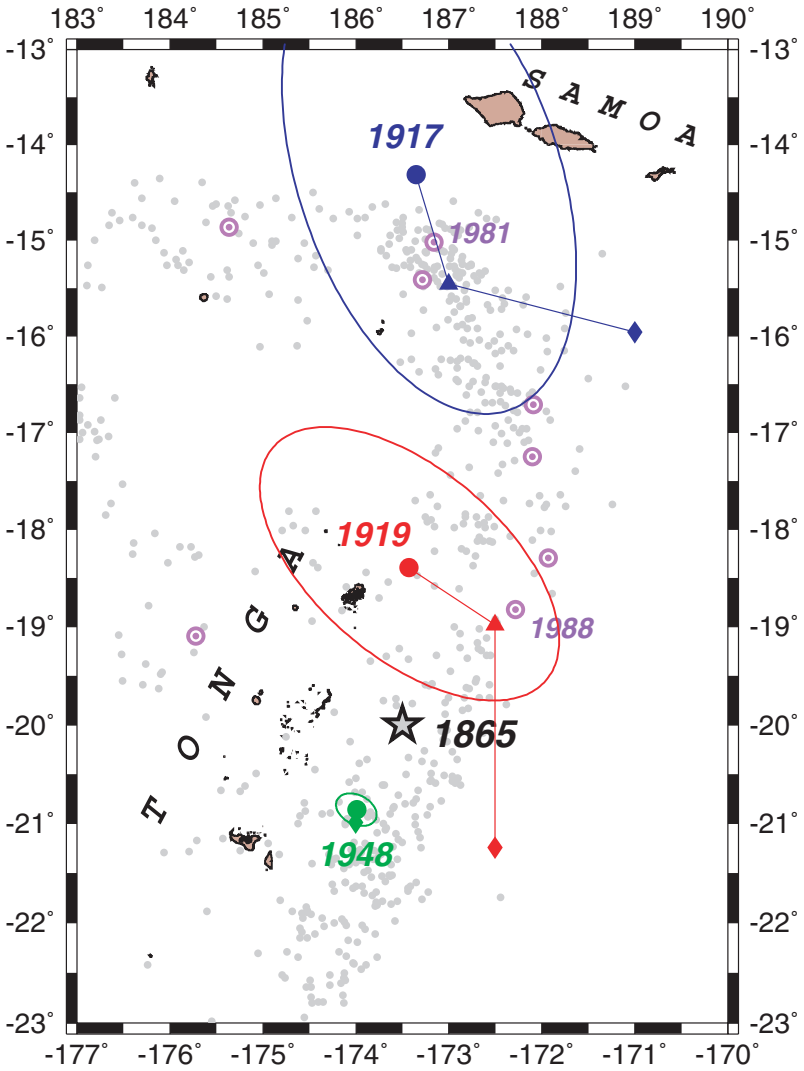

Figure 2. Relocation of three instrumental-era historical earthquakes (1917 June 26, 1919 April 30, 1948 September 8). For each event, the solid dot is the relocated epicentre, the diamond shows the reported ISS epicentre, and the triangle the location from Gutenberg & Richter (1954). The Monte Carlo ellipses are computed for Gaussian noise with standard deviations $\sigma_G = 15$ s (1917, 1919) and 3 s (1948). The grey dots in the background are all CMT solutions shallower than 50 km, with those with $M_0 \geq 10^{26}$ dyn cm shown as bull's-eye symbols; the 1981 and 1988 earthquakes discussed in the text are identified. The star is the probable location of the 1865 event.

• *1917 June 26.* This event relocates to 14.37°S; 173.35°W (Fig. 2), based on 13 retained *P* times, with a standard deviation $\sigma = 3.21$ s, a remarkably low figure for an earthquake this old; however, hypocentral depth cannot be resolved. The Monte Carlo ellipse intersects the northern cusp of the plate boundary, suggesting that the true location of the earthquake may be around 15°S, 173.2°W, close to the epicentral estimate of Gutenberg & Richter (1954), and also to the earthquake of 1981 September 1, which featured normal faulting. It is most improbable that the 1917 event expressed direct subduction of Pacific lithosphere. Its tsunami was destructive in Samoa, but at most decimetric in the far field (Solov'ev & Go 1984).

• *1919 April 30.* Based on a data set of 20 traveltimes, we relocate this earthquake to 18.42°S, 173.43°W, with a standard deviation $\sigma = 4.76$ s. This location is significantly west of the plate boundary, nearly under the arc, and the relocated epicentre is at the western limit of the belt of shallow (<50 km) seismicity; the few large ($M_0 > 10^{26}$ dyn cm) events in the modern CMT database are about 120 km to the ESE, which could suggest a deeper than normal focus for the 1919 event. However, the Monte Carlo ellipse is elongated in the WNW–ESE direction and intersects the belt of modern seismicity. The 1919 earthquake could thus be either a regular subduction event at 19°S, 172.5°W, or a slightly deeper earthquake ($h \approx 60$ km) at our relocated epicentre; we note that large modern intraplate earthquakes are documented at such depths in the Tonga arc (Christensen & Lay 1988; Lundgren & Okal 1988). The 1919 traveltime data set cannot resolve hypocentral depth, and thus both solutions will be tested in our simulations.

• *1948 September 8.* This more modern event is very well constrained. We use 71 traveltimes to relocate it at 20.87°N, 173.99°W, with a standard deviation $\sigma = 3.00$ s; this epicentre essentially coincides with the ISS location (21°S, 174°W), and the Monte Carlo ellipse semi-major axis is only 24 km. A moderate tsunami did not exceed 10 cm in Samoa (Solov'ev & Go 1984). We estimate the moment of this event at only 3×10^{27} dyn cm, based on mantle magnitude measurements at Pasadena and San Juan.

3.1 Other events

In the immediate vicinity of the probable source of the 1865 event, Gutenberg & Richter (1954) report a large earthquake on 1902 February 9, at 20°S, 174°W, to which they assign $M = 7.8$. Since this event pre-dates the systematic reporting of phases by the ISS, it is impossible to relocate; no tsunami is reported by Solov'ev & Go (1984).

Between the 1948 epicentre at 21°S and the Louisville Ridge subduction point at 25.5°S, there are no known shallow earthquakes with any reported magnitude greater than 7.2, with the exception of the event of 1982 December 19 at 24.1°S ($M_s = 7.7$), which is characterized by an anomalously slow source (Newman & Okal 1998; Okal *et al.* 2003). As such, this shock is a so-called 'tsunami earthquake', as defined by Kanamori (1972), but it remains a small event ($M_0 = 2 \times 10^{27}$ dyn cm) and its tsunami was only centimetric at Papeete (Talandier & Okal 1989).

By contrast, south of the Louisville Ridge, the character of the subduction changes; it has long been recognized that the slab becomes substantially steeper (Sykes 1966), but larger interplate thrust earthquakes are documented, such as the second event in the doublet on 1976 January 14 ($M_0 = 8.2 \times 10^{27}$ dyn cm), which generated a tsunami reaching 90 cm in Fiji (Solov'ev *et al.* 1986). The large Kermadec earthquake of 1917 May 1 also fits this pattern, although our relocation is only mediocre, at 29.42°S, 179.08°W ($\sigma = 7.73$ s), with a large Monte Carlo ellipse whose semi-major axis approaches 300 km. The occurrence of larger events south of the Louisville Ridge may be related to the presumably younger age of the plate, due to the large offset along the Eltanin Fracture Zone, even though it is unclear exactly how long this feature has been present along the Pacific–Antarctic Ridge or its predecessors (Molnar *et al.* 1975).

To conclude this section, the picture emerging from the review of historical seismicity in Tonga is that of a segment rupturing in large earthquakes (comparable to the 1919 event) north of 20°S, and of a regime of smaller events south of 21°S. The latter could express the slower convergence rate in the southern part of the Tonga arc (Bevis *et al.* 1995), resulting in reduction in seismic coupling, and in the maximum size of interplate earthquakes. It would then be probable that the rupture zone of the 1865 earthquake extended approximately 180 km between those of the 1919 and 1948 events; in Figs 1 and 2, we use a probable epicentre at 20°S, 173.5°W. This is essentially the model proposed in Fig. 1 (p. 9) of Solov'ev & Go (1984), although the origin of their estimates of rupture lengths is unknown. The scaling laws of Geller (1976) (his eq. (15)) would then predict that the 1865 earthquake may have had a moment of about 4×10^{28} dyn cm, for a stress drop $\Delta\sigma = 50$ bar.

An alternative end-member scenario would assume that the whole southern Tonga arc from 20°S to 24°S ruptured during the 1865 earthquake, over a length of 550 km. This interpretation would be supported by the report of the event being felt at sea by the S.S. *Syrene* at 24°S; 173.5°W (Rudolph 1887). The 1865 source region would presently constitute a seismic gap undergoing only relatively moderate events, such as the 1948 shock. A similar alternation in the regime of stress release between mega-events and merely large ones has been documented in other strongly coupled subduction systems, such as in southern Peru or the Nankai Trough (Ando 1975; Dorbath *et al.* 1990). In this scenario, and with a moment of 7×10^{29} dyn cm, the 1865 event would be comparable in size to the 1964 Alaskan earthquake (Kanamori 1970), and should have generated a truly catastrophic transoceanic tsunami. We will confirm in Section 4 that this scenario is unrealistic for the 1865 shock, given the relatively moderate character of the tsunami observed at Rarotonga and Nuku Hiva; however, the possibility of such mega-events in Tonga cannot be totally excluded.

4 HYDRODYNAMIC SIMULATIONS

In this section, we carry out simulations for a number of source scenarios of the 1865 earthquake, with the goal of matching quantitatively the observations analysed in Section 2, namely a run-up of about 2 m in Avarua and 0.8 m in Taiohae. As detailed in Table 1, we consider four models of the 1865 earthquake, with moments ranging from 1.5×10^{28} to 2×10^{29} dyn cm; as we will see, the latter value is already excessive, and thus we do not consider even larger sources. We also consider two models of the 1919 source, in an attempt to explain the absence of far-field reports for its tsunami.

Following the methodology developed in a number of previous studies (e.g. Synolakis *et al.* 2002; Borrero *et al.* 2003), our modelling efforts involve several steps: first we use a model of seismic dislocation to infer the static displacement of the ocean floor through the algorithm of Geller (1976) with a rigidity of 5×10^{11} dyn cm^{-2}. The hydrodynamic simulation is then performed using the MOST (method of splitting tsunami) code (Titov & González 1997; Titov & Synolakis 1998), with the static deformation field as an initial condition of the hydrodynamic problem; this is legitimate because seismic deformations always occur much faster than water waves would propagate out of the deformed area.

In the case of a pre-instrumental earthquake, we obviously have no information on the focal mechanism, and for this reason we simply use a pure 45°-dipping thrust fault on a plane striking N198°E, i.e. in the azimuth of the Tonga trench. Note that this mechanism, which is essentially the CMT solution for the nearby event of 1988 October 8 ($\phi = 196°$, $\delta = 43°$, $\lambda = 90°$), expresses the tectonic interplate motion at the subduction zone. We consider a hypocentral depth of 25 km, and scale the dimensions of the source with the seismic moments considered.

Table 1. Parameters and results of models used in hydrodynamic simulations.

Model number	Seismic moment (dyn cm)	Source depth (km)	Fault length (km)	Fault width (km)	Fault slip (m)	Rarotonga		Taiohae	
						Deep water (m)	Run-up (m)	Deep water (m)	Run-up (m)
				1865 simulation					
1	4×10^{28}	25	177	88	5.2	0.4	2.20	0.08	0.58
2	8×10^{28}	25	223	111	6.6	0.6	3.10	0.11	0.75
3	2×10^{29}	25	302	151	8.9	1.15	5.20	0.20	0.95
4	1.5×10^{28}	25	127	64	3.75	0.21	1.00	0.04	0.32
				1919 simulation					
5	2.5×10^{28}	25	151	76	4.45	0.30	1.40	0.06	0.40
6	2.5×10^{28}	60	151	76	4.45	0.12	0.70	0.03	0.23

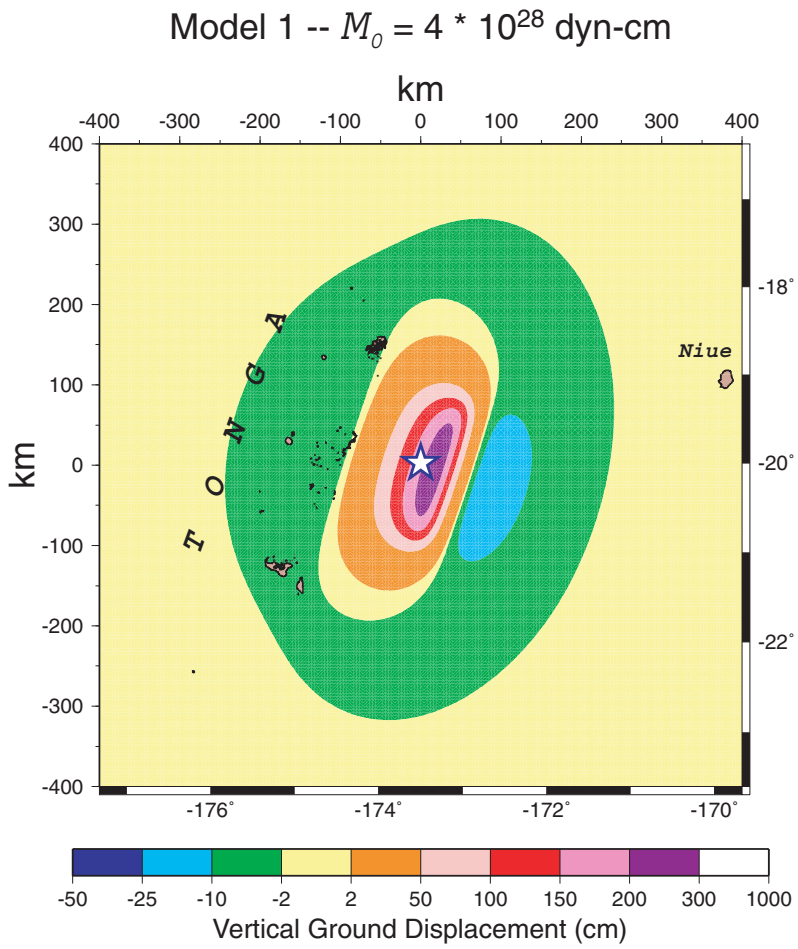

Figure 3. Ground displacement computed from the Okada (1985) algorithm for Model 1, and used as an initial condition for our numerical simulation.

MOST solves the non-linear shallow-water wave equations using a variable staggered grid with the method of fractional steps; a full description is given in Synolakis (2002). Our simulations are carried out in a region extending from 5°S to 20°S and from 180° to 140°W, using the 2-min bathymetric grid of Smith & Sandwell (1997). In the vicinity of the receiving shores, the grid is refined using available marine charts.

We detail here our best-fitting model, 'Model 1', featuring a moment of 4×10^{28} dyn cm. The fault zone is taken as 177 by 88 km, the upward limit of rupture as 25 km and the slip on the fault as 5.2 m, corresponding to a shear strain of 10^{-4} across the width of the fault; it also fits eq. (15) of Geller (1976) with $\Delta\sigma = 50$ bar and $\mu = 5 \times 10^{11}$ dyn cm^{-2}. As shown in Fig. 3, the static displacement field reaches a maximum of 2.3 m, 120 km ESE of the Tonga arc. On the islands themselves, the vertical displacement is no more than a few centimetres, which would not have resulted in a detectable change in permanent sea level. Fig. 4 presents a map of the maximum water surface elevation reached by the tsunami in our simulation area. The lobe of strong amplitudes radiated in the direction perpendicular to the Tonga arc (E20°S) is a classical example of directivity due to source finiteness (Ben-Menahem & Rosenman 1972), while the enhanced amplitudes in the Line Islands and farther away along the direction N30°E are the result of refraction and focusing by the shallow waters of the Manihiki Plateau at 12°S, 163°W, an effect discussed for example by Woods & Okal (1987).

At Rarotonga, the computation on the coarse grid is stopped at isobath 1000 m, 5 km from the shoreline, where the zero-to-peak amplitude of the wave is found to be 40 cm (Fig. 5a), and a new grid with a final sampling of 50 m is used to simulate the propagation of the waves and their run-up into Avarua and Avatiu harbours (Fig. 6a). The topography of the shoreline is modelled only along a 3-km stretch of coast, corresponding to the detailed close-up chart on New Zealand marine chart number 9558. As shown in Fig. 7(a), the amplitude of run-up is modelled consistently between 1.5 to 2 m, with peak values reaching 2.5 m in the river estuaries at Avarua and Avatiu. Given the fragmentary nature of the available report, we regard this modelling as satisfactory.

At Nuku Hiva, the computation on the coarse grid is stopped at isobath 1500 m, where the zero-to-peak amplitude is only 8 cm (Fig. 5b). A smoothed bathymetry duplicating the average gradient is then used to propagate the wave to the entrance of the bay, whose response is modelled using a 50-m grid, digitized from French Navy nautical chart number 7352 (Fig. 6b). As shown in Fig. 7(b), the amplitude of the wave increases strongly in the bay, with run-up ranging from 50 to 60 cm at the back of the bay. These numbers are somewhat lower than the value of the observed run-up (80 cm) estimated from the correspondence of Lawson (1869), but the agreement is acceptable. Note in particular the strong amplification (by roughly one order of magnitude) between the amplitude of the tsunami at the 1000-m isobath (Fig. 5b) and the run-up at the back of Taiohae Bay, which agrees well with the Hébert *et al.* (2001) simulation of

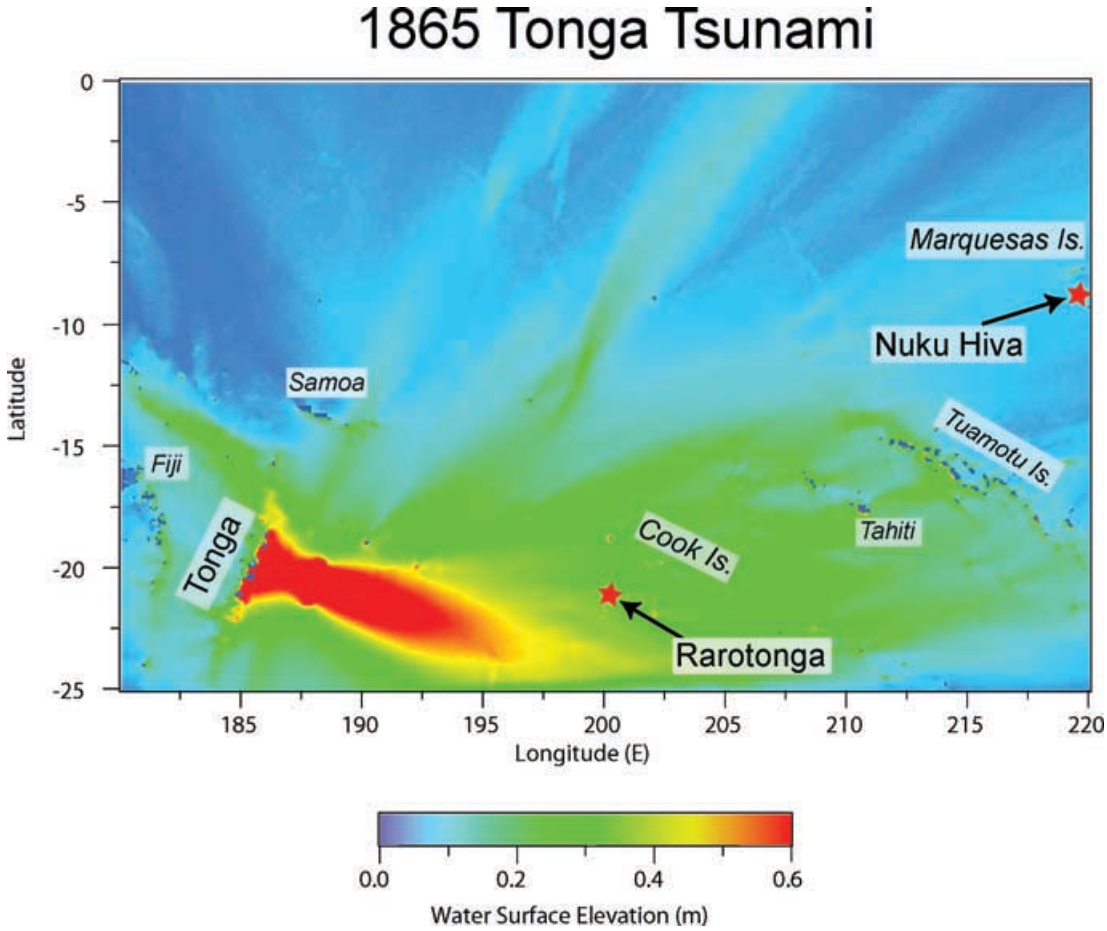

Figure 4. Maximum amplitude of the tsunami wave on the high seas, as simulated by MOST under Model 1 and the coarse grid. Note the strong directivity lobe perpendicular to the Tonga trench, and the local focusing effects of bathymetric features. The stars show the locations of Rarotonga in the Cook Islands and of Nuku Hiva in the Marquesas chain.

more recent trans-Pacific tsunamis in the Marquesas. This level of amplification is also in very general agreement with the empirically based law used by Ward & Asphaug (2003).

4.1 Other sources

We similarly tested the run-up at Rarotonga and Nuku Hiva for several models with varying values of the seismic moment, from 1.5×10^{28} to 2×10^{29} dyn cm, with source parameters obtained from scaling laws (Geller 1976). Results are shown in Fig. 7. In the case of the smaller event (Model 4), run-up at Rarotonga reaches only 80 cm, with a peak of 1 m in the river bed. At low tide, the sea level would not exceed the high-tide mark; if the tide was high, the down-draw would not have exposed the bay noticeably below low water. We regard this model as falling short of the reported inundation. On the other hand, Models 2 and 3 lead to excessive run-ups of 3 and 5 m respectively, which would probably have inflicted serious damage to shoreline structures, of which there are no reports in the various historical sources. With this in mind, we consider such sources as clearly too large, and deem unnecessary the modelling of even larger earthquakes (M_0 up to 7×10^{29} dyn cm), which would involve rupturing the entire Northern Tonga subduction zone.

The results at Taiohae are less clear-cut, due to the combination of lesser deep-water amplitudes at this more distant island located outside the directivity lobe from Tonga (Fig. 4), and greater tidal range, which adds to the uncertainty in the reported run-up. Nevertheless, we can rule out the smaller source (Model 4), which predicts only a small wave (of 30 cm run-up), unlikely to reach the high-water mark, except during a very high tide.

Finally, we explore in Models 5 and 6 the tsunami generated by the 1919 earthquake, for which there are no reports in Rarotonga and the Marquesas. The seismic moment of this earthquake is reasonably well constrained, at about 2.5×10^{28} dyn cm (Okal 1992). We first test Model 5 in which the earthquake is located at a normal depth in the interplate seismic belt; we use the same focal mechanism as for the 1865 event. We obtain an average run-up of 1.4 m (Fig. 7a), which might have been detected if the tide had been high, as suggested by modern tidal calculations. By contrast, in Model 6, we place the earthquake deeper and below the arc. The average run-up becomes only 70 cm, less than maximum high tide. Given the night-time occurrence (the 1919 tsunami is expected in Rarotonga at 22:40 local solar time), the run-up predicted by Model 6 would probably have gone undetected; on this basis, we express a slight preference for interpreting the 1919 earthquake as occurring under the arc, in the geometry of Model 6. At Taiohae, both models predict very small run-ups (40 and 23 cm respectively; Fig. 7b), confirming that the tsunami should have gone unnoticed, especially in darkness (the wave being expected at 03:00 local solar time).

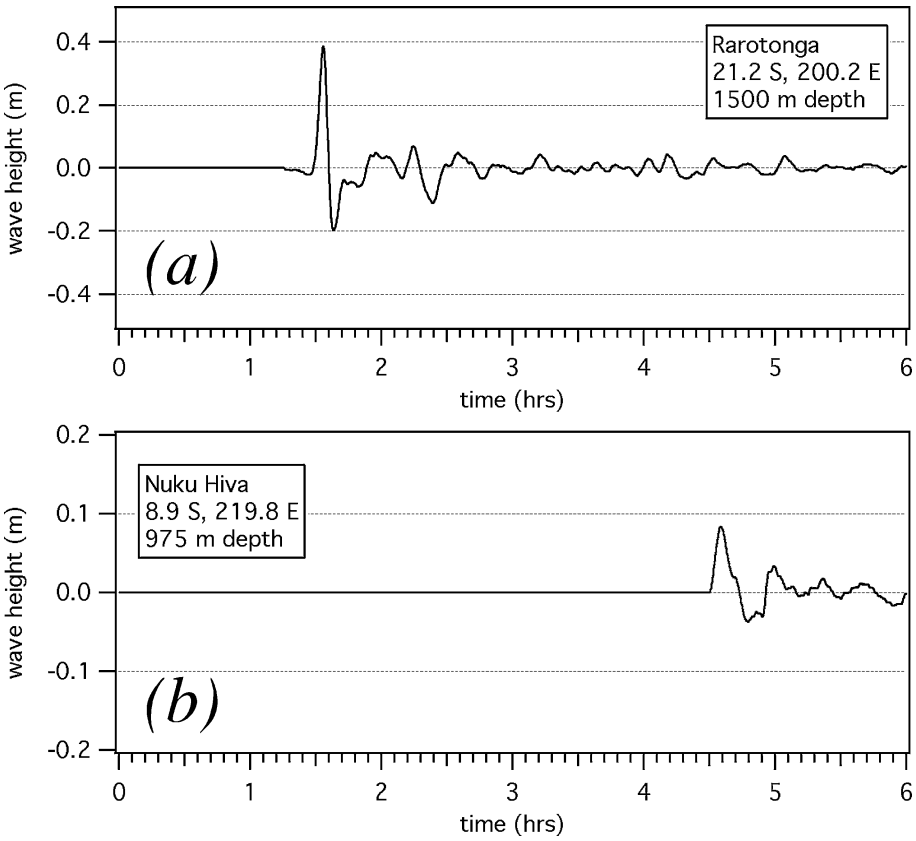

Figure 5. Amplitude of the tsunami wave simulated under Model 1 at deep-water gauges located off Rarotonga (a) and Taiohae Bay, Nuku Hiva (b). These time series are used as input to the fine-grid computations of run-up shown on Fig. 7.

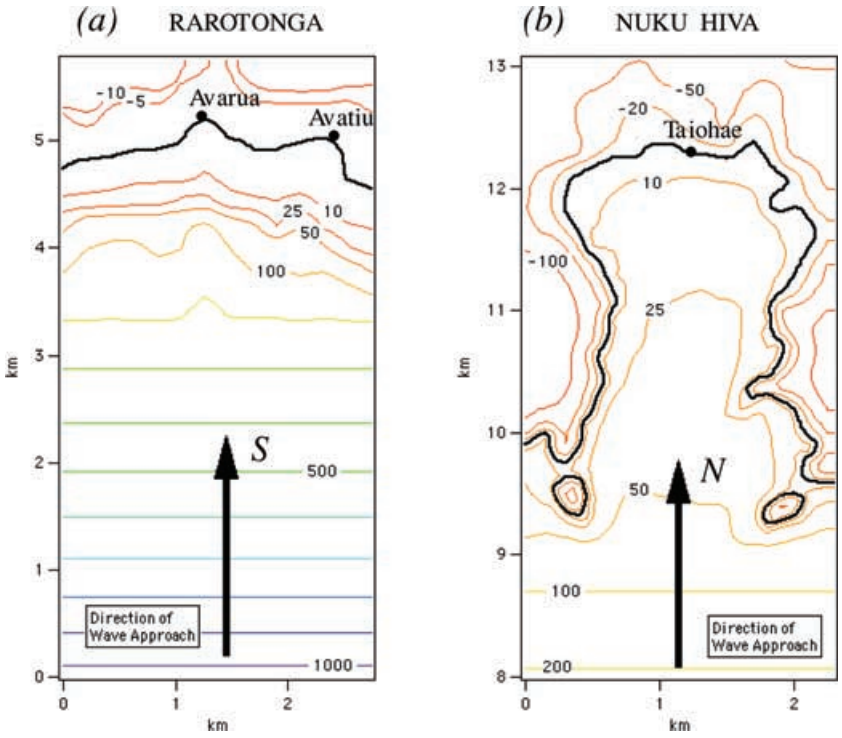

Figure 6. Maps of the receiving shores at Rarotonga (a) and Nuku Hiva (b), showing the localities mentioned in the text. The shore is shown as the thick line. Isobaths beyond 100 m are at 100 m intervals, with numbers showing depth in metres; negative numbers on shore indicate positive elevation above sea level. The map at Rarotonga is oriented southwards up.

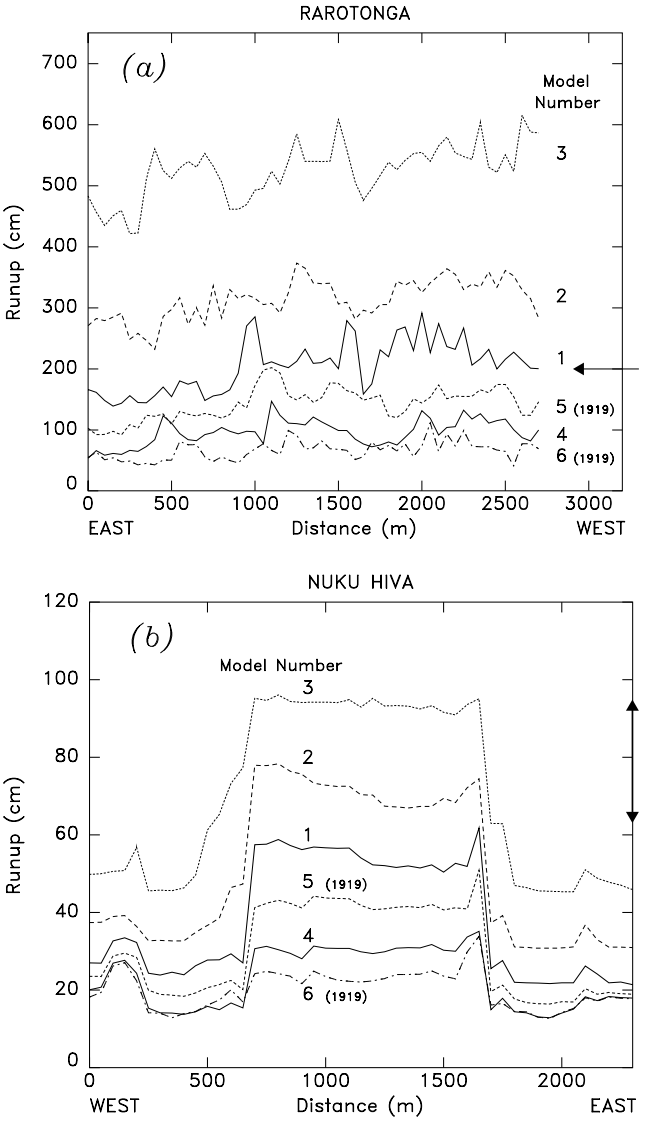

Figure 7. (a) Profiles of run-up at Rarotonga for the various models simulated in this study, and listed in Table 1. The abscissa is distance along the shoreline in the E–W direction (see Fig. 6a). The preferred model (1) is shown by the solid line. The arrow shows the value of the estimated 1865 run-up at Avarua; there is no report at Rarotonga for the 1919 tsunami. (b) Same as (a) for Taiohae, Nuku Hiva. The abscissa is distance along the W–E direction (see Fig. 6b). Note the strong amplification effect of the narrow Taiohae Bay. The range of possible values for the run-up at Taiohae is shown by the arrows on the right.

5 CONCLUSION

Numerical hydrodynamic simulations of the reported run-ups of the 1865 Tonga earthquake at two far-field locations require a moment on the order of 4×10^{28} dyn cm. This figure also agrees with the scale of the felt area, as estimated from the few available historical reports. In particular smaller seismic sources, comparable to the largest earthquakes documented during the instrumented historical period, would only generate minor tsunamis, with little or no potential for human detection, let alone damage. We also suggest that the large 1919 event may have occurred under the arc, at a greater than normal depth, which would help explain the absence of far-field reports of its tsunami.

The 1865 episode is of crucial importance for the assessment of tsunami risk in the Cook Islands, and more generally in the south-central Pacific. A repeat of the 1865 wave taking place at high tide would reach more than 2 m above the high-water mark, which in modern days could inflict significant damage to harbour and shore infrastructure. The scenario establishes that Tonga does carry the potential threat of generating a destructive far-field tsunami, and the variability observed in the sequence of rupture at other subduction zones leaves open the possibility of even larger events along the Tonga arc. Such a risk should be taken into account as part of tsunami warning and mitigation procedures for the Cook Islands, French Polynesia and other island groups in the southcentral Pacific, especially given the shorter traveltime of tsunami waves from Tonga, as compared with other tsunamigenic zones around the Pacific.

ACKNOWLEDGMENTS

Maps were drawn using the GMT software (Wessel & Smith 1991). We are deeply indebted to Jean-Louis Teuruarii Candelot who pointed out the correspondence of Lawson (1869), and more generally shared with us his erudition on the history of the Marquesas. We thank Hal Mofjeld for a customized computation of the tide at Rarotonga. The paper benefited from constructive reviews by Kenji Satake and Eric Geist, and from the comments of editor Steve Ward. This research was supported by the National Science Foundation under grants CMS-00-99333 and CMS-03-01081 (to CES), and CMS-03-01054 (to EAO).

REFERENCES

Abe, K., 1981. Magnitudes of large shallow earthquakes from 1904 to 1980, *Phys. Earth planet. Inter.,* **27,** 72–92.

Adams, C.J., 1983. Age of the volcanoes and granite basement of the Auckland Islands, Southwest Pacific, *N.Z. J. Geol. Geophys.,* **26,** 227–237.

Ando, M., 1975. Source mechanism and tectonic significance of historical earthquakes along the Nankai rough, Japan, *Tectonophysics,* **27,** 119–140.

Angenheister, G., 1921. Beobachtungen an Pazifischen Beben; ein Betrag zum Studium der obersten Erdkruste, *Nachriten von der Königl. Gesellschaft der Wissenschaften zu Göttingen, Mathematisch-Physikalische Klasse,* 2–25.

Anonymous, 1987. Underwater volcano erupts, shaking ship of researchers, *New York Times,* pp. A1 and A22, 1987 October 14.

Barry, J.M., 1866. On submarine earthquakes and volcanoes, *Dublin Q. J. Sci.,* **6,** 197–204.

Ben-Menahem, A. & Rosenman, M., 1972. Amplitude patterns of tsunami waves from submarine earthquakes, *J. geophys. Res.,* **77,** 3097–3128.

Bevis, M. *et al.*, 1995. Geodetic observations of very rapid convergence and back-arc extension at the Tonga Arc, *Nature,* **374,** 249–251.

Borrero, J.C., Bu, J., Saiang, C., Uslu, B., Freckman, J., Gomer, B., Okal, E.A. & Synolakis, C.E., 2003. Field survey and preliminary modeling of the Wewak, Papua New Guinea earthquake and tsunami of September 9, 2002, *Seismol. Res. Letts.,* **74,** 393–405.

Christensen, D.H. & Lay, T., 1988. Large earthquakes in the Tonga region associated with subduction of the Louisville Ridge, *J. geophys. Res.,* **93,** 13 367–13 389.

Cullen, D.J., 1969. Quaternary volcanism at the Antipodes Islands: its bearing on structural interpretation of the southwest Pacific, *J. geophys. Res.,* **74,** 4213–4220.

Dorbath, L., Cisternas, A. & Dorbath, C., 1990. Assessment of the size of large and great historical earthquakes in Peru, *Bull. seism. Soc. Am.,* **80,** 551–576.

Fuchs, C.W.C., 1866. Die vulcanischen Erscheinungen im Jahre 1865, *Neues Jahrbuch für Mineralogie, Geologie und Paläontologie,* pp. 523–557, Stuttgart.

Geller, R.J., 1976. Scaling relations for earthquake source parameters and magnitudes, *Bull. seism. Soc. Am.,* **66,** 1501–1523.
Gutenberg, B. & Richter, C.F., 1954. *Seismicity of the Earth,* 310 pp, Princeton University Press, Princeton, NJ.
Hébert, H., Heinrich, P., Schindelé, F. & Piatanesi, A., 2001. Far-field simulation of tsunami propagation in the Pacific Ocean: impact on the Marquesas Islands (French Polynesia), *J. geophys. Res.,* **106,** 9161–9177.
Kanamori, H., 1970. The Alaska earthquake of 1964: radiation of long-period surface waves and source mechanism, *J. geophys. Res.,* **75,** 5029–5040.
Kanamori, H., 1972. Mechanisms of tsunami earthquakes, *Phys. Earth planet. Inter.,* **6,** 346–359.
Krümmel, O., 1911. *Handbuch der Ozeanografie,* Vol. 2, J. Engelhorn, Stuttgart.
Lawson, W.T., 1869. *Correspondence to Rev. S. Damon,* Bishop Museum Archives, Honolulu.
Lundgren, P.R. & Okal, E.A., 1988. Slab decoupling in the Tonga arc: the June 22, 1977 earthquake, *J. geophys. Res.,* **93,** 13 355–13 366.
Molnar, P., Atwater, T., Mammerickx, J. & Smith, S.M., 1975. Magnetic anomalies, bathymetry and the tectonic evolution of the South Pacific since the Late Cretaceous, *Geophys. J. R. astr. Soc.,* **40,** 383–420.
Newman, A.V. & Okal, E.A., 1998. Teleseismic estimates of radiated seismic energy: The E/M_0 discriminant for tsunami earthquakes, *J. geophys. Res.,* **103,** 26 885–26 898.
Okada, Y., 1985. Surface deformation due to shear and tensile faults in a half-space, *Bull. seism. Soc. Am.,* **75,** 1135–1154.
Okal, E.A., 1992. Use of the mantle magnitude M_m for the reassessment of the seismic moment of historical earthquakes. I: Shallow events, *Pure appl. Geophys.,* **139,** 17–57.
Okal, E.A., Alasset, P.-J., Hyvernaud, O. & Schindelé, F., 2003. The deficient *T* waves of tsunami earthquakes, *Geophys. J. Int.,* **152,** 416–432.
Perrey, A., 1867. Note sur les tremblements de terre en 1865, avec supplément pour les années antérieures de 1843 à 1864, Mémoires couronnés de l'Académie Royale des Sciences et des Belles-Lettres, **19,** 125 pp, Bruxelles.
Ruff, L.J. & Kanamori, H., 1980. Seismicity and the subduction process, *Phys. Earth planet. Inter.,* **23,** 240–252.
Rudolph, E., 1887. Über submarine Erdbeben und Eruptionen, *Gerlands Beiträge zur Geophysik,* **1,** 133–365.
Smith, W.H.F. & Sandwell, D.T., 1997. Global sea floor topography from satellite altimetry and ship depth soundings, *Science,* **277,** 1956–1962.
Solov'ev, S.L. & Go, Ch.N., 1984. Catalog of tsunamis on the eastern shore of the Pacific Ocean, *Can. Transl. Fisheries Aquat. Sci.,* **5078,** 285 pp, Sidney, BC.
Solov'ev, S.L., Go, Ch.N. & Kim, Kh.S., 1986. *Katalog Tsunami v Tikhom Okeane, 1969–1982 gg.*, 164 pp, Nauka, Moscow [in Russian].
Synolakis, C.E., 2002. Tsunami and seiche, in, *Earthquake Engineering Handbook,* pp. **9**-1–**9**-90, eds Chen, W.-F. & Scawthorn, C., CRC Press, Boca Raton, FL.
Synolakis, C.E., Bardet, J.-P., Borrero, J.C., Davies, H.L., Okal, E.A., Silver, E.A., Sweet, S. & Tappin, D.R., 2002. The slump origin of the 1998 Papua New Guinea tsunami, *Proc. R. Soc. Lond.,* A., **458,** 763–789.
Sykes, L.R., 1966. The seismicity and deep structure of island arcs, *J. geophys. Res.,* **71,** 2981–3006.
Talandier, J. & Okal, E.A., 1989. An algorithm for automated tsunami warning in French Polynesia, based on mantle magnitudes, *Bull. seism. Soc. Am.,* **79,** 1177–1193.
Titov, V.V. & González, F.I., 1997. Implementation and testing of Method Of Splitting Tsunami (MOST) model, *NOAA Technical Memorandum ERL-PMEL,* **112,** 11 pp, for sale by National Technical Information Service, Springfield, VA.
Titov, V.V. & Synolakis, C.E., 1998. Numerical modeling of tidal wave runup, *J. Wtrwy. Port Coast. Engng.,* **B124,** 157–171.
Uyeda, S. & Kanamori, H., 1979. Back-arc opening and the mode of subduction, *J. geophys. Res.,* **84,** 1049–1061.
Ward, S.N. & Asphaug, E., 2003. Asteroid impact tsunami of 2880 March 16, *Geophys. J. Int.,* **153,** F6–F10.
Wessel, P. & Smith, W.H.F., 1991. Free software helps map and display data, *EOS, Trans. Am. geophys. Un.,* **72,** 441, 445–446.
Woods, M.T. & Okal, E.A., 1987. Effect of variable bathymetry on the amplitude of teleseismic tsunamis: a ray-tracing experiment, *Geophys. Res. Lett.,* **14,** 765–768.
Wysession, M.E., Okal, E.A. & Miller, K.L., 1991. Intraplate seismicity of the Pacific Basin, 1913–1988, *Pure appl. Geophys.,* **135,** 261–359.

APPENDIX: THE CASE OF THE *ORIENT*

Barry (1866) reports an intriguing incident, involving the convict ship *Orient* being rocked at sea, as if 'grating over a ledge of rocks', while sailing back from Adelaide to London around Cape Horn. This episode is relevant to the present study since its date is given as 1865 November 17, at 7.20 a.m. It is unclear if and when calendars would have been reset on a ship crossing the date line, but there is at least some possibility that the incident took place concurrently with the Tonga earthquake, i.e. within a window of a few hours. While the location of the occurrence is given as 51.73°S, 170.82°E (see Fig. 1a), in the southern part of the Campbell Plateau, it remains somewhat confused, as the report also mentions that, at the time of the incident, the Auckland Islands bore northeast 210 miles. This could be a simple typographic error, the islands being about that distance northwest of the reported site, or the longitude of the site may be erroneous, e.g. the true value could be 160.82°E.

At any rate, we discard an association of this incident with the Tonga earthquake, based on the following remarks: at either of the possible locations, the epicentral distance is more than 34°, a range at which body waves are felt only under exceptional circumstances; we note that there are no reports of the event being felt in New Zealand, at roughly half the distance. We also do not expect surface waves with dominant periods probably around 20 s, corresponding to wavelengths of ∼100 km, and at most millimetric amplitudes, to affect a ship measuring less than 50 m, and sailing at sea. In addition, and irrespective of the fact that we do not know of any report of a surface vessel 'feeling' *T* waves, we note that any such phases (which the 1865 event most probably generated) would have been blocked to the possible two locations of the ship, either by New Zealand, or by an 800-km path across the Chatham Rise and over the Campbell Plateau, which constitute a notorious mask for hydroacoustic propagation. Finally, the *Orient* could not have felt the tsunami itself for several reasons: except under shoaling conditions, the combination of amplitudes and wavelengths of a tsunami wave will allow a 50-m ship to simply ride the wave unaffected, in the manner of a cork on the surf; we note that soundings by the crew failed to reveal a shallow ground (Barry 1866). In addition, the tsunami would take at least 7 hr to propagate over or around the shallow, and thus slow, Campbell Plateau to the reported location of the incident, reaching it around noon, solar time, which regardless of the exact time being kept on the ship could not be estimated as 7:20 a.m., as reported by Barry (1866).

We conclude that the incident on board the *Orient* was unrelated to the Tongan earthquake. Its exact nature remains a mystery; the theory of a volcanic origin, suggested by Barry (1866), would be supported by some similarities with more recent events (Anonymous 1987), and by the absence of damage on the ship's hull, as later inspected in dry dock, but would be difficult to reconcile with the absence of discoloration of the surface of the sea, and with the grating nature of the disturbance of the ship. We also note that even though the various islands in the area are volcanic in nature with some as recent as 0.25 Ma (Cullen 1969), the youngest units are found to the east of the Campbell Plateau, and there are no

reports of present-day volcanism (Adams 1983). It is more probable that the rocking of the *Orient* was the result of a localized phenomenon, such as a rogue wave, possibly generated by a local underwater landslide, and totally unrelated to the earthquake and tsunami 3800 km to the northeast. At the westernmost possible location (161°E), the ship could have felt an earthquake on the Macquarie Ridge plate boundary, once again unrelated to the Tonga event.